

Automatic segmentation editing for cortical surface reconstruction

Xiao Han, Chenyang Xu*, Maryam E. Rettmann, and Jerry L. Prince

The Johns Hopkins University, Baltimore, MD 21218, USA

ABSTRACT

Segmentation and representation of the human cerebral cortex from magnetic resonance images is an important goal in neuroscience and medicine. Accurate cortical segmentation requires preprocessing of the image data to separate certain subcortical structures from the cortex in order to generate a good initial white-matter/gray-matter interface. This step is typically manual or semi-automatic. In this paper, we propose an automatic procedure that is based on a careful analysis of the brain anatomy. Following a fuzzy segmentation of the brain image, the method first extracts the ventricles using a geometric deformable surface model. A region force, derived from the cerebrospinal membership function, is used to deform the surface towards the boundary of the ventricles, while a curvature force controls the smoothness of the surface and prevents it from growing into the outer pial surface. Next, region-growing identifies and fills the subcortical regions in each cortical slice using the detected ventricles as seeds and the white matter and several automatically determined sealing planes as boundaries. To make the method robust to segmentation artifacts, a putamen mask drawn in the Talairach coordinate system is also used to help the region growing process. Visual inspection and initial results on 15 subjects show the success of the proposed method.

Keywords: cortical surface reconstruction, automated image segmentation, geometric deformable surface, brain atlas, subcortical structures, MRI brain images

1. INTRODUCTION

Segmentation and representation of the human cerebral cortex from magnetic resonance images is an important goal in neuroscience and medicine. This procedure is required for quantification of the geometry and geometric variations across populations, visualization of functional data, and surgical planning. This task is difficult not only because of the complexity of brain anatomy but also because of limitations in the imaging process — e.g., image noise, intensity inhomogeneities, and partial volume effects.

In recent years, there has been a great amount of work dedicated to the development of accurate and automatic cortical surface reconstruction methods [1–4]. The success of these methods typically relies on expert knowledge and assumptions about the structure of the brain cortex. For example, it is usually assumed that the brain cortex consists of a convoluted sheet of gray matter (GM) encasing the white matter (WM), and that the cortical surface has the topology as a sphere. To make these assumptions more valid, preprocessing is required to separate the subcortical gray matter structures, such as the caudate nucleus and the putamen, from the cortical GM in order to seal the opening at the brain stem.

In past work, our group has developed a highly automatic procedure for reconstructing the central layer of the entire human cerebral cortex. In this method, after segmenting the brain area into its three compartments: gray matter (GM), white matter (WM) and cerebrospinal fluid (CSF), a manual editing is performed on the WM volume to fill regions corresponding to the ventricles and subcortical GMs before an isosurface algorithm can be used to extract the true GM/WM interface. This manual step is tedious and time-consuming, which prevents the overall method from being used in brain studies involving large numbers of data sets.

In this paper, we present an automatic procedure that replaces manual editing. The procedure was developed by combining a thorough understanding of the brain anatomy with some carefully designed, largely heuristic, algorithms. In the next section, we begin by summarizing the whole cortical surface reconstruction procedure. We then describe the automatic cortical preprocessing procedure in detail. Section 3 presents some results and provides an evaluation of the proposed method. Section 4 concludes the paper.

Send correspondence to Jerry L. Prince at jprince@jhu.edu.

* Present address: Siemens Corporate Research, Princeton NJ 08648, USA.

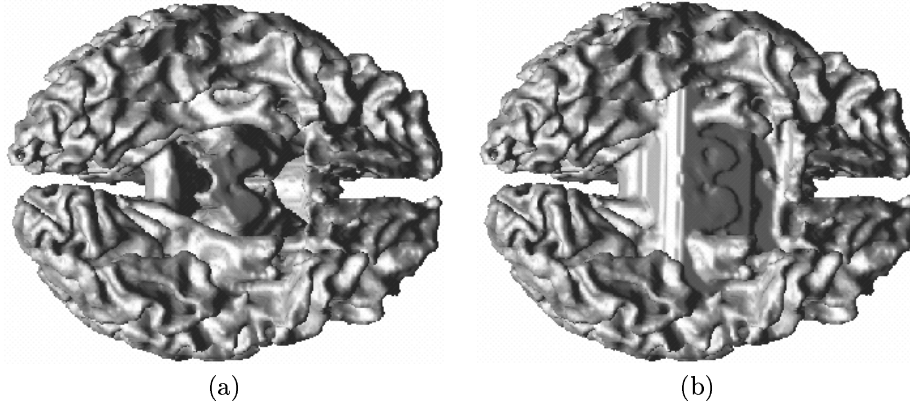


Figure 1. The GM/WM interface obtained from the original (a) and the edited (b) WM segmentation.

2. METHODS

In the following, we first summarize the whole procedure for getting a surface representation of the central layer of the cortex, which also serves as the context of the automatic filling method. We then continue to describe our automatic method of editing the WM volume to remove the extraneous structures.

2.1. Cortical surface reconstruction algorithm

The method reported in [2] has the following four major steps. First, the raw T1-weighted MR images are preprocessed to remove extracranial tissues. The dura, marrow, skin, cerebellum, and part of the brain stem are removed in this step. Each volume is then interpolated to isotropic voxels. Second, the brain image volume is segmented into fuzzy membership functions comprising the GM, WM, and CSF [5, 6]. The use of fuzzy segmentation offers robustness to noise and partial volume effect and removes the dependency on raw image intensity in later steps. Third, an iterative process comprising median filtering and isosurface generation on the WM membership function produces an initial estimate of the GM/WM interface. This step produces an initial estimate of the gray-matter surface that has the correct topology of a sphere. Finally, a deformable surface algorithm moves the initial surface towards the central layer of the cortex yielding the final reconstructed cortical surface.

Since the boundaries of the ventricle and subcortical GM such as the putamen and the caudate nucleus are generally connected to the cortical GM/WM interface in the WM membership function, the isosurface computed from the WM membership function is a composite of the cortical GM/WM interface and these extraneous connected surfaces (see Fig. 1(a)). To resolve this problem, the original method requires a manual step to fill the ventricle and subcortical GMs regions in the segmented WM volume before applying the median filters and the isosurface algorithm. The manual step is tedious and time-consuming, and must be automated for extensive use.

2.2. Overview of automatic editing

The main observation that serves as the basis of the proposed method is that the subcortical GM together with the ventricles form concavities inside the WM that open towards the bottom of the brain, around the brain stem area. Ideally, if we could find a suitable “sealing plane,” and perform a region growing operation inside the WM, we would be able to fill these concavities, thus separating the subcortical GM and ventricles from the cortex (see Fig. 1(b)).

The concavities that must be filled can be identified by the presence of the ventricles. To make use of this anatomical information, we first extract the ventricles using a 3D geometric deformable surface model. Then, using the detected ventricles as seeds and the segmented WM and one or more automatically determined sealing planes as boundaries, the concavities in the WM volume are filled by region-growing.

While this overall approach is conceptually valid, two key difficulties arise, which requires modification to the details. First, because of the irregular shape of the brain, it is generally not possible to find a single “sealing plane” for a three-dimensional (3D) region growing to work properly. Instead, we found that it is possible to apply this same principle on two-dimensional (2D) coronal slices, separately, and then merge these results into a 3D result. In this case, “sealing lines” are identified at the base of the brain within each coronal slice.

A second difficulty may arise when the thin strand of WM that exists between the putamen and the cortical GM is broken due to a segmentation error. This causes the region-growing procedure to fail. We address this problem by applying a mask to identify the putamen region. The mask is drawn *a priori* in Talairach coordinates and is mapped automatically to each individual brain after the brain is registered with the atlas.

In the following sections, we explain each step of the procedure in detail.

2.3. Registration to the Stereotactical Coordinate System

We register the brain to the Talairach coordinate system using the method described in [7]. The registration only requires user to pick two landmark points: the anterior (AC) and the posterior commissure (PC). Registration to this stereotactic system is always needed for other reasons in the overall brain processing procedure, and is thus not an additional cost within the WM editing process.

As mentioned above, a putamen mask is drawn (once) in Talairach coordinates. This mask is then mapped to the individual brain using the transformation obtained in this registration step.

2.4. Extraction of the Ventricles

We apply a geometric deformable surface model to extract the ventricle. The geometric active contour/surface models for image segmentation were proposed independently by Caselles et al. [8] and Malladi et al. [9]. Based on the theory of curve evolution and implemented using the level-sets numerical algorithm, these models provide several advantages over traditional parametric deformable surface models in that they are completely intrinsic and thus independent of the parametrization of the evolving surface. They are also relatively insensitive to the initialization, and can automatically handle changes in topology such as the surface merging and splitting. We first introduce the basic concepts of the geometric deformable models and then present the particular speed function we designed for the finding the boundaries of the ventricle.

Let $Q = [0, a] \times [0, b] \times [0, c]$ and $I : Q \rightarrow R^+$ be a given 3D image volume. In the geometric deformable surface model, the surface S is embedded as the zero level set of a four-dimensional (4D) function $\Psi : Q \times R \rightarrow R^+$, and moves implicitly through the temporal evolution of the level set function Ψ . This description corresponds to an Eulerian formulation of the surface motion, rather than the Lagrangian description of the traditional parametric deformable model. Since Ψ is defined on the image lattice and updated at fixed grid points, no parameterization of the surface is needed. Topological changes are automatic since the surface can merge or split while Ψ keeps to be a well-defined function. At any time instant, the current surface location $S(t)$ can be obtained by taking the zero level-set of the function $\Psi(x, t)$: $S(t) = \{x : \Psi(t, x) = 0\}$. Usually, Ψ is taken to be the signed distance function to the surface with negative value inside the surface and positive outside, which can be computed efficiently by the Fast Marching method [10].

In the original formulation, the following equation is proposed to solve the active image segmentation problem:

$$\Psi_t = g(k + v) \|\nabla \Psi\|, \quad (1)$$

where k is the mean curvature of the evolving surface and is given by $\text{div}(\nabla \Psi / \|\nabla \Psi\|)$, v is a constant, and g is a stopping term, which is defined as:

$$g(x) = \frac{1}{1 + \|\nabla G_\sigma(x) * I(x)\|}. \quad (2)$$

The diffusive term $k\|\nabla \Psi\|$ has the effect of smoothing the front, while the hyperbolic term $v\|\nabla \Psi\|$ either shrinks or expands the surface depending on the sign of v . The deformation of the active surface is coupled with the image data through the multiplicative stopping term $g(x)$, which is near zero at strong edges. These terms are also called the speed terms of the geometric deformable surface model.

To apply this technique to our segmentation problem of finding the ventricle, we use a slight modification of the original geometric deformable model. Instead of using a constant speed term v , we allow v to be spatially-varying both in magnitude and sign. The ventricle is classified as CSF in T1-weighted images, so we define $v(x)$ to be

$$v(x) = 2\mu_{CSF}(x) - 1, \quad (3)$$

where $\mu_{CSF}(x)$ is the fuzzy membership function of the CSF class. Since $\mu_{CSF}(x) \in [0, 1]$, $v(x)$ lies in the range of $[-1, 1]$. Clearly, if the surface is outside of the ventricle, $\mu_{CSF} < 0.5$ and v is negative, then the surface shrinks



Figure 2. Surface rendering of the detected ventricle.

towards the boundary of the ventricle; if the surface is inside, v is positive, and the surface will expand. At the boundaries, $\mu_{CSF} = 0.5$ and $v = 0$, the movement of the surface is controlled only by the curvature term.

From the above analysis, we note that the stopping term $g(x)$ is no longer needed. Instead, we use the following evolution equation:

$$\Psi_t = (w_k k + v) \|\nabla \Psi\|, \quad (4)$$

where the weight w_k controls the relative strength of the different speed terms, and balances between fidelity to the boundary and smoothness of the surface. The speed term $v(x)$ in Eq. (3) corresponds to a regional force, which is often desirable when reliable region information is available [11].

Fig. 2 shows one example of an extracted ventricle. We want to point out that the automatic editing algorithm does not require a very accurate segmentation of the ventricle. As can be seen from the figure, some external cisterns, the superior cistern and its continuous the transverse fissure, are always included in the segmentation since they are connected to the third ventricle. These external cisterns only appear in posterior coronal slices, and we have a simple algorithm to separate them from the true posterior ventricle horns when it is necessary. This issue is discussed in more detail later.

CSF exists both within the ventricles and around the outside of the brain cortex. To extract only the boundaries of the ventricles, we initialized our deformable surface model inside the WM, and used a relatively high curvature force to prevent the surface from growing into the outer pial surface (the interface between the CSF and the cortical GM). In our experiments, we chose the weight $w_k = 0.5$ for all data sets. Since the connections between the ventricle and the outer CSF are thin and weak, we have found that the results are not sensitive to the exact value of w_k .

The segmentation results are also quite robust to the initialization. The only requirement is that the initial surface must intersect the ventricles but not the pial surface. It would be relatively straightforward to initialize the surface in Talairach coordinates and transform it to the current brain. However, we found such an elaborate initialization unnecessary. Instead, we initialized the deformable surface model using a small circular ball centered at the centroid of the CSF membership function. A possible drawback of this small initial surface is that it will take longer to converge to the desired boundary than a more carefully selected initialization. To compensate, we use the so-called *narrow band* implementation of the geometric deformable model, as described in [9].

The deformable surface model guarantees that the extracted boundaries are closed surfaces. By thresholding the final distance function at the zero value, we can assign each voxel of the image volume as either inside (the distance being negative) or outside (positive distance) the ventricle boundary. Voxels inside or on the boundary surface, i.e. belonging to the ventricle, are used as seeds in the following region growing procedures. These (ventricle) voxels are also used to determine which coronal slices must be edited, as will become clear later.

2.5. Fill the Ventricle and the Subcortical Gray Matter

The regions corresponding to the ventricle and the subcortical GM are part of the background in the binarized WM volume. The goal of editing is to identify these regions and fill them as if they were WM. We use region-growing for this purpose. It is carried out in 2D coronal slices both for simplicity and to allow the lower “sealing” boundary to vary from anterior to posterior. In coronal views, these special regions form C-shaped concavities with the opening facing towards the bottom of the brain (see Fig. 4). Thus, the main task is to define suitable horizontal sealing lines

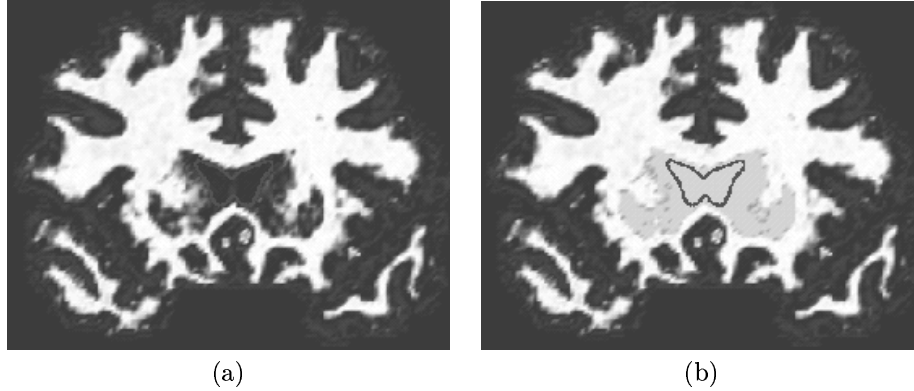


Figure 3. A coronal slice that gets correctly filled during the first pass. The dark curves show the detected ventricle boundary.

to stop the region-growing operation from leaking into the true background. In the most posterior slices, where the two hemispheres are separated in the segmented WM volume, region-growing must be performed in each hemisphere individually.

One particular problem sometimes arises due to segmentation error. From the anatomy of the brain, the putamen is separated from the cortical GM by a thin layer of WM. However, voxels in this region are sometimes misclassified as GM, which results in the putamen being connected to the subcortical GM. This wrong connection produces handles on the boundary surface of the segmented WM, which is the wrong topology. This demonstrates one important reason for this initial WM editing procedure. The bridge between the putamen and the cortical GM can cause failure in the region growing process. Although this problem does not always happen, to make the editing algorithm robust to segmentation artifacts, we apply a pre-drawn mask to identify the putamen region. The putamen mask is a simple rectangular box drawn on the Talairach atlas and mapped to the current brain volume after the brain is registered to the Talairach coordinate system. The mask covers the extent of the left and right putamens.

Overall, the WM filling procedure begins with a binary WM volume (a binarized WM membership function), and then runs three consecutive passes of region growing which fills all the background regions corresponding to the detected ventricle and the subcortical GM. Slices fail to be filled during the first pass will be processed again in the second pass, and so on. We now describe each pass in detail.

First Pass. The first pass is the simplest. In each 2D coronal slice, region growing is used to find all background holes, and to fill them with WM if they contain part of the detected ventricle. Background holes are defined to be connected components of background pixels that are not adjacent to the image boundary. This pass correctly fills the anterior slices that do not pass through the brain stem. Some posterior slices are also filled correctly if the ventricle regions form closed holes inside the WM. Fig. 3 shows one coronal slice that is correctly edited after the first pass.

The coronal slices in the center of the brain are not changed after the first pass because in this range the ventricle and subcortical GM are topologically connected to the slice boundary through the opening around the brain stem area. For these slices, a horizontal sealing line must be defined for each slice to provide a lower boundary for region growing. This is the task of the second pass.

Second Pass. The second pass starts by examining each coronal slice to see whether unfilled regions of ventricle pixels exist. For each slice that remains to be filled, the algorithm tries to select a horizontal sealing line to separate the subcortical regions from the rest of the background. One reasonable choice is to make the lines be aligned with the bottom of the diencephalon. Again, we could select a single sealing plane in the Talairach coordinate system and map it to the subject brain, which automatically defines a sealing line for each slice. In the current implementation, however, we adopt a more data-driven approach in which a line is selected separately for each slice and is aligned with the “bottom” of the GM along the mid-sagittal line in the current slice. * More specifically, we search along

*The mid-sagittal line is the intersection of the coronal slice and the mid-sagittal plane, i.e./ the sagittal plane that passes through the AC-PC line.

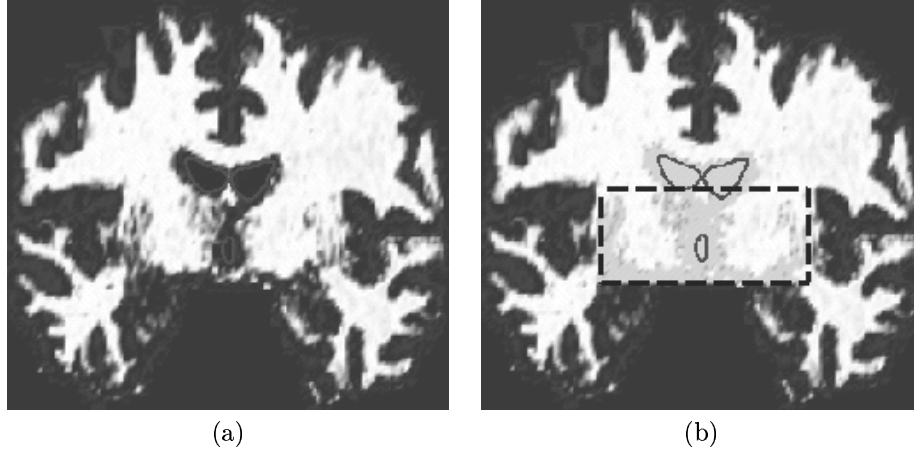


Figure 4. (a) The original WM slice and (b) the edited result (WM filled). The dark curves show the detected ventricle boundary and the dashed rectangular box shows the boundary of the putamen mask.

the mid-sagittal line in the current slice from the bottom to the top until the first GM pixel is encountered. The horizontal sealing line is then defined to be passing through this point. Since the cerebellum and the brain stem were removed during the initial preprocessing step, the line found this way is roughly aligned to the bottom of the diencephalon.

In case the putamen is connected to the cortical GM, we now fill the region covered by the putamen mask, and then perform the usual constrained region growing to fill the remaining concavities in these slices. The region-growing is stopped by either the WM boundary or the additional sealing line. Fig. 4 shows the editing result on a mid-ranged coronal slice. It is clear that the putamen mask is necessary to limit the region growing.

Third Pass. The first two passes correctly fill most of the coronal slices except some posterior ones that are behind the PC, where the segmented WM separates into two disjoint hemispheres. In these slices, we have to address the two hemispheres separately, which is the task of the third pass.

In these posterior slices, the regions that need to be filled correspond to the posterior horns of the ventricle, since there is no more subcortical GM. These ventricular regions might already be correctly filled during the first pass if they form closed holes inside the WM. As mentioned above, some external cisterns (the superior cistern and the transverse fissure) are present in these slices and they need not be filled. Thus, in order to determine which slices still need to be processed, we first need to separate the external cisterns from the true ventricle horns in these slices.

One feature that can differentiate the ventricle horns from the external cistern is location: the external cistern lies around the mid-sagittal plane, while the ventricle horns lie separately in the two hemispheres. We extract the cistern in these slices by picking a ventricle-labeled point in the mid-sagittal line as a seed and then region-grow from it (in 2D) until all the ventricle-labeled voxels connected to it are relabeled as non-ventricle. The remaining ventricle-labeled voxels are considered to belong to the true ventricle horns. After separating the cistern from the true ventricle, we search for unfilled ventricle horns in the left and right hemisphere separately. If unfilled regions exist, they become the seeds for the third-pass region growing.

To fill the ventricle horn in either hemisphere, two sealing lines are usually required, one horizontal and one vertical. The position of the horizontal line is determined in the following way. First, draw a vertical line through each voxel that is labeled as ventricle. Then search along each line towards the bottom of the brain until a WM voxel is encountered. Next, among all the WM voxels found in the second step, take the one with the lowest vertical coordinate and draw a horizontal line passing through this point. The position of the vertical line is taken to be aligned with the rightmost (leftmost) boundary of the ventricle horn in the left (right) hemisphere. We then shift the vertical planes towards the mid-sagittal plane by 3 pixels in order to fill a bit more around the ventricle horns.

With the two lines as additional boundary, the region growing can successfully fill the regions occupied by the posterior ventricle horns. Fig. 5 shows one posterior coronal slice and the corresponding edited result.

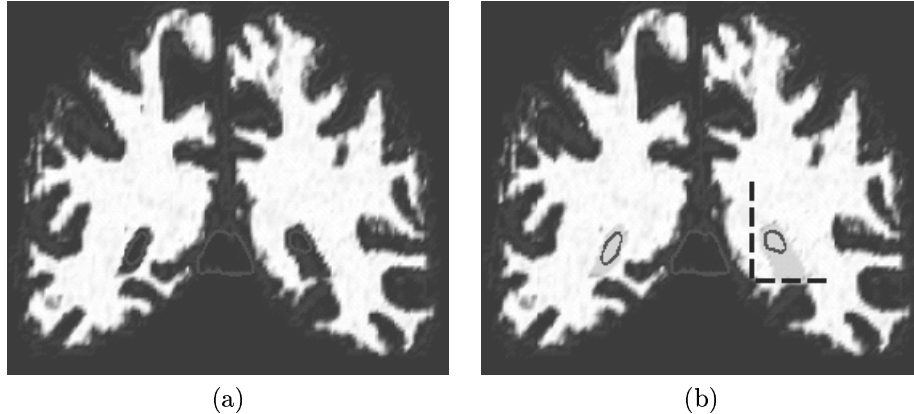


Figure 5. One posterior slice of the segmented WM volume (a) and its corresponding editing result (b). The dashed lines show the sealing planes found for the right hemisphere.

2.6. Summary of WM editing

The three passes of region growing complete the automatic editing procedure. If we take the isosurface of the edited WM volume, the boundaries of the ventricle and subcortical GM are no longer connected to this surface. Furthermore, in cases in which the putamen is connected to the cortex in the initial segmentation, the edited WM volume will not contain a large handle in the putamen area. This is a further advantage of this method.

3. RESULTS AND DISCUSSIONS

We tested the proposed method on 15 T1-weighted MR brain images obtained from the Baltimore Longitudinal Study on Aging [12]. The images have a size of $256 \times 256 \times 196$ voxels. The results were assessed by experts through visual inspection of the cross-sections and 3D renderings of the extracted WM-GM interface. The results showed that the ventricle detection method is reliable and that automatic editing of the WM is consistent with what experts would do. There were no anomalous omissions or fills, and the extraneous boundaries of the ventricle and the subcortical gray matter structures were successfully disconnected from the cortical surface.

To obtain quantitative measure of performance, we compared the automatically edited result with the manually edited result in the next step of cortical surface extraction: topology correction. The automatic approach reported in [2] uses a succession of median filters applied to the edited WM membership function until the topology of a calculated isosurface is correct. Table 1 lists the numbers of median filters required to correct the topology of the 15 brains using both the automatic and manual initializations. We observe from Table 1 that the automatic editing usually requires more median filters. One reason for this discrepancy is that manual editing is performed extremely carefully, and is sometimes repeated in order to reduce the number of required median filters. Another reason is that the median filter is not an optimal topology correction method. Some handles are difficult for the median filter to remove, and it can sometimes create new handles.

One region that often poses difficulties for the median filter is the area around the hippocampus, where the WM is quite entangled with the GM. To avoid this problem, the operator performing manual editing often removes some WM in this area. The automatic editing algorithm does not deal with the hippocampus region explicitly, and the large number of median filters thus required produce over-smoothed initial surface that is unacceptable. To overcome this problem, we recently developed a new topology correction algorithm, the Graph-Based Topology Correction Filter (GTCF), to correct the topology of the edited WM volumes [13]. It is similar in principle to the method developed by Shuttack and Leahy [14, 15]. This new method removes handles locally and efficiently, and thus eliminates the need to explicitly deal with the hippocampus area. Experiments have shown that it gives better results than the median filter (Compare Table 2 with Table 4 and Table 3 with Table 5).

To assess the influence of the automatic editing algorithm on the accuracy of our cortical surface reconstruction algorithm, we computed ten landmark errors on the final reconstructed central surfaces, and compared them with the previous results reported in [2], which were obtained using manual editing. Landmark errors were computed on

Table 1. Number of median filters required to get the correct topology.

Subject	S1	S2	S3	S4	S5	S6	BA	DA	DJ	DM	DN	DO	DX	DZ	DW
Manual Editing	3	9	8	9	7	3	4	12	7	8	7	9	9	5	11
Automatic Editing	6	12	18	14	16	3	8	14	6	10	12	13	9	8	9

Table 2. Landmark errors of using the manual editing and median filters (in mm).

Sulcus	Subject						Mean	Std
	1	2	3	4	5	6		
CS ₁	1.21	2.40	1.48	0.22	0.63	0.47	1.10	0.80
CS ₂	1.67	1.84	0.86	1.17	1.27	2.02	1.50	0.44
PCG ₁	0.77	0.66	0.34	0.64	1.27	0.67	0.73	0.30
PCG ₂	0.84	0.96	0.93	0.67	0.40	0.35	0.69	0.27
TLG ₁	0.34	0.60	2.90	0.93	2.80	0.47	1.30	1.20
TLG ₂	3.50	2.12	0.98	1.25	5.73	1.29	2.50	1.80
CALC ₁	0.82	0.68	1.31	0.25	0.38	0.68	0.69	0.37
CALC ₂	1.25	5.73	2.92	0.63	2.24	0.39	2.20	2.00
MFG ₁	0.32	0.75	0.66	1.38	0.34	0.45	0.65	0.40
MFG ₂	1.37	1.35	0.64	0.23	1.01	1.06	0.94	0.44
Mean	1.20	1.70	1.30	0.74	1.60	0.78	–	–
Std	0.91	1.60	0.91	0.43	1.70	0.53	–	–

six of the fifteen brains, and the results are summarized in the following tables (Table 2–5). It is shown in the results that the automatic editing procedure works well with the other procedures of the cortical surface reconstruction method. It produces small landmark errors except in the cases that a large number of median filters are required to generate the topologically correct initial surface. As shown in the last two tables, if the new topology correction algorithm is used, the automatic editing and the manual method produce almost indistinguishable final results, and they are much better than the results when using the median filter.

Compared with about one hour of manual editing, the automatic method takes only 30 minutes of computer time on an SGI Onyx2 workstation with a 250-MHz, R10000 processor. Typically, 25 minutes of the total time is spent on the extraction of the ventricles, and the rest is spent on registering the putamen mask and the region growing procedures. There is still much room to improve the speed of the geometric deformable surface method — for example, using multiscale techniques.

Table 3. Landmark errors of using the automatic editing and median filters (in mm).

Sulcus	Subject						Mean	Std
	1	2	3	4	5	6		
CS ₁	1.20	2.43	3.85	0.25	0.60	0.23	1.43	1.44
CS ₂	1.68	1.98	4.37	2.10	4.32	2.13	2.76	1.24
PCG ₁	0.91	0.96	0.30	0.69	2.06	0.56	0.91	0.61
PCG ₂	0.94	0.65	1.39	0.59	0.60	0.32	0.75	0.37
TLG ₁	0.34	0.53	2.35	0.91	1.39	0.43	0.99	0.77
TLG ₂	3.46	5.21	1.63	0.97	2.35	0.87	2.42	1.67
CALC ₁	0.86	0.79	1.33	0.41	3.56	0.72	1.28	1.16
CALC ₂	1.38	6.08	3.04	0.73	4.42	0.44	2.68	2.25
MFG ₁	0.32	0.53	0.80	1.40	1.38	0.48	0.82	0.47
MFG ₂	1.45	1.22	0.49	0.17	0.70	1.02	0.84	0.48
Mean	1.25	2.04	1.96	0.82	2.14	0.72	–	–
Std	0.89	2.01	1.41	0.58	1.49	0.55	–	–

Table 4. Landmark errors of using the manual editing and GTCF filters (in mm).

Sulcus	Subject						Mean	Std
	1	2	3	4	5	6		
CS ₁	1.15	2.43	1.03	0.21	0.49	0.17	0.91	0.46
CS ₂	1.81	1.69	0.81	1.07	1.12	1.83	1.39	0.45
PCG ₁	0.75	0.70	0.23	0.59	2.08	0.48	0.81	0.35
PCG ₂	0.92	0.52	0.56	0.65	0.52	0.46	0.61	0.37
TLG ₁	0.61	0.57	0.41	1.07	0.70	0.41	0.63	0.39
TLG ₂	0.44	2.18	1.05	0.92	0.32	1.09	1.00	0.42
CALC ₁	0.90	0.68	1.21	0.35	0.32	0.70	0.69	0.42
CALC ₂	1.30	4.32	2.04	0.76	1.97	0.49	1.81	0.47
MFG ₁	0.31	0.32	0.28	1.40	1.38	0.58	0.71	0.47
MFG ₂	1.33	1.11	0.51	0.19	0.59	0.86	0.77	0.44
Mean	0.95	1.45	0.81	0.72	0.95	0.71	–	–
Std	0.46	1.25	0.55	0.40	0.66	0.47	–	–

Table 5. Landmark errors of using the automatic editing and GTCF filters (in mm).

Sulcus	Subject						Mean	Std
	1	2	3	4	5	6		
CS ₁	1.15	2.43	1.03	0.21	0.39	0.15	0.89	0.47
CS ₂	1.80	1.72	0.81	1.08	1.25	2.08	1.46	0.47
PCG ₁	0.75	0.70	0.24	0.59	2.09	0.84	0.87	0.38
PCG ₂	0.92	0.51	0.56	0.63	0.50	0.40	0.59	0.40
TLG ₁	0.60	0.56	0.41	1.08	0.94	0.17	0.63	0.43
TLG ₂	0.44	2.18	1.05	0.91	0.43	0.88	0.98	0.45
CALC ₁	0.89	0.68	1.21	0.42	0.29	0.72	0.70	0.45
CALC ₂	1.46	4.00	2.05	0.61	2.05	0.51	1.78	0.51
MFG ₁	0.31	0.32	0.28	1.40	1.39	0.55	0.71	0.47
MFG ₂	1.33	1.11	0.51	0.19	0.58	0.89	0.77	0.43
Mean	0.97	1.42	0.82	0.71	0.99	0.72	–	–
Std	0.47	1.17	0.55	0.40	0.68	0.55	–	–

4. CONCLUSION

We proposed an automatic method to replace a time-consuming, manual step in our cortical surface reconstruction procedure. This makes the whole procedure suitable for large numbers of studies. Consistency and reproducibility should be better using this procedure, and these will be evaluated in an ongoing study. Initial results show very good results using the described procedure within the entire cortical surface reconstruction procedure.

ACKNOWLEDGMENTS

This work was partially supported by the NSF ERC/CISST#9731748 and by the NIH/NINDS R01NS37747 and a Whitaker Foundation graduate fellowship.

REFERENCES

1. G.J. Carman, H.A. Drury, and D.C. Van Essen, "Computational methods for reconstruction and unfolding the cerebral cortex," *Cerebral Cortex* **5**, pp. 506–517, 1995.
2. C. Xu, D. L. Pham, M. E. Rettmann, D. N. Yu, and J. L. Prince, "Reconstruction of the human cerebral cortex from magnetic resonance images," *IEEE Transactions on Medical Imaging* **18**(6), pp. 467–480, 1999.
3. A.M. Dale, B. Fischl, and M.I. Sereno, "Cortical surface-based analysis i: Segmentation and surface reconstruction," *NeuroImage* **9**, pp. 179–194, 1999.
4. B. Fischl, M.I. Sereno, and A.M. Dale, "Cortical surface-based analysis ii: Inflation, flattening, and a surface-based coordinate system," *NeuroImage* **9**, pp. 195–207, 1999.
5. D. L. Pham and J. L. Prince, "An adaptive fuzzy c-means algorithm for images segmentation in the presence of intensity inhomogeneities," *Pattern Recognition Letters* **21**(1), pp. 57–68, 1999.
6. D. L. Pham and J. L. Prince, "An adaptive fuzzy segmentation algorithm for three-dimensional magnetic resonance images," in *Lecture Notes in Computer Science: Information Processing in Medical Imaging*, IPMI'99, (Visegád, Hungary), June/July 1999.
7. D. Lemoine, C. Barillot, B. Gibaud, and E. Pasqualini, "An anatomical-based 3d registration system of multimodality and atals data in neurosurgery," in *Lecture Notes in Computer Science*, vol. 511, (Springer-Verlag, Berlin), 1991.
8. V. Caselles, R. Kimmel, and G. Sapiro, "Geodesic active contours," *International Journal of Computer Vision* **22**, pp. 61–79, 1997.
9. R. Malladi, J.A. Sethian, and B.C. Vemuri, "Shape modeling with front propagation: A level set approach," *IEEE Transactions on Pattern Analysis and Machine Intelligence* **17**(2), pp. 158–175, 1995.
10. J. Sethian, "A fast marching level set method for monotonically advancing fronts," *Proceedings of the National Academic of Sciences* **93**, pp. 1591–1595, 1996.
11. C. Xu, A. Yezzi, and J. Prince, "On the relationship between parametric and geometric active contours," in *Asilomar Conference*, (USA), 2001.
12. S. Resnick, A. Goldszal, C. Davatzikos, S. Golski, M. Kraut, E. Metter, R. Bryan, and A. Zonderman, "One-year age changes in mri brain volumes in older adults," *Cerebral Cortex* **10**, pp. 464–72, May 2000.
13. X. Han, C. Xu, U. Braga-Neto, and J. Prince, "Graph-based topology correction for brain cortex segmentation," in *Submitted to the 2001 Conference on Image Processing for Medical Imaging*, (San Diego, USA), 2001.
14. D. Shattuck and R. Leahy, "Topological refinement of volumetric data," in *Proceedings of the SPIE*, vol. 3661, pp. 204–213, (San Diego, USA), February 1999.
15. D. Shattuck and R. Leahy, "Topologically constrained cortical surfaces from mri," in *Proceedings of the SPIE*, vol. 3979, pp. 747–758, (San Diego, USA), February 2000.